Doubly-fed Induction Generator in Frequency Domain

Marco Köhler, Robert Dimitrovski

Institute of Electrical Energy Systems
Friedrich-Alexander-University of Erlangen-Nuremberg
Erlangen, Germany
maarkoe@gmail.com

Abstract— **In this paper, an impedance based frequency domain model of a doubly fed induction generator is developed. The machine is simplified so that it can be viewed as it's thévenin impedance. The resulting model is used for stability simulations.**

Index Terms— *doubly fed induction generator, Impedance model, frequency domain, thévenin impedance, wind turbine generator, simulation*

I. INTRODUCTION

With climate change and the move to renewable energy, the way energy is created changes as well. New ways to generate electricity often need new ways to optimize the use of generators. Doubly fed induction generators (DFIG) play out their advantages in modern wind turbines. Those generators are relatively new in the electrical grid and therefore they can have different impacts than traditional induction machines. To keep control over the power generation, DFIGs effects on the grid should be calculated different from other generators and so new models are needed to integrate the generator in stability considerations.

II. DEVELOPMENT OF FREQUENCY DOMAIN IMPEDANCE MODELL

A. Impedance model basics

An impedance model is used to build a doubly fed induction generator model in frequency domain. This method is often used to determine stability of electrical systems [1] [2].

The goal is to find the Thévenin equivalent impedance of the whole machine. The System then can be displayed in a simple circuit with a voltage source and an impedance like seen in Figure 1 [3].

Not all influences will be taken care of in this model. The DFIG consists of an induction generator that has its rotor connected to a voltage source converter. This converter is connected to the grid via a separate transformer. The wind rotor is connected to the generator with a gearbox. The masses included have a two-mass swing system which consists mainly out of the wind rotor and the generator rotor masses. Those masses and swing frequencies are ignored when calculating the Thévenin impedance [4].
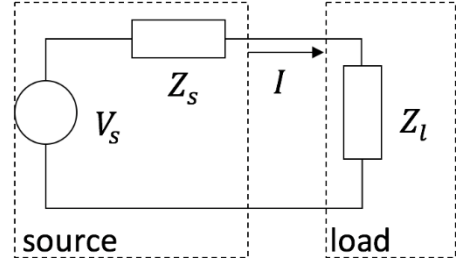

Figure 1 Thévenin impedance circuit model

Figure 2 shows the components of a typical DFIG where its rotor is connected to a voltage source converter. Only electrical elements will be included in the Impedance calculation. The RSC and GSC controller parameter will have an influence on the equivalent impedance and therefore cannot be neglected.

The stator winding of the induction generator is connected to the three-phase grid voltage and frequency ω_s. The resulting magnetomotive force (MMF) of the windings is (1-3) [4]:

$$\Theta_a(\delta, t) = N i_a(t) \cos \delta \tag{1}$$

$$\Theta_b(\delta, t) = N i_b(t) \cos(\delta - \frac{2\pi}{3}) \tag{2}$$

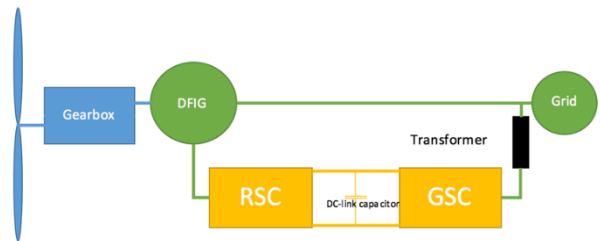$$\Theta_c(\delta, t) = N i_c(t) \cos(\delta + \frac{2\pi}{3}) \tag{3}$$
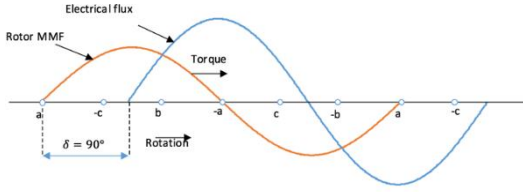

Figure 2 Doubly fed induction machine components

Figure 3 MMF and Flux waveforms

Figure 4 Space vector circuit model

With N being the windings count, δ the air gap angle and sinusoidal currents (4-6). Figure 3 shows the waveforms. The phase windings are marked with *a*, *b* and *c*.

$$i_a(t) = I \cos \omega_s t \qquad (4)$$

$$i_b(t) = I \cos(\omega_s t - \frac{2\pi}{3}) \qquad (5)$$

$$i_c(t) = I \cos(\omega_s t + \frac{2\pi}{3}) \qquad (6)$$

Adding the phase MMFs together can be simplified if all three phases are sinusoidal with a phase difference of 120° leads to (7):

$$\Theta_{ges}(\delta, t) = \frac{3}{2} NI \cos(\delta - \omega_s t) \qquad (7)$$

B. Circuit Model development

To develop a one circuit model, the currents and voltages are transformed into space vector [5]. The resulting MMF, and Voltage for the stator and rotor circuit becomes (8-9) [6]:

$$\vec{V}_s = R_s \vec{I}_s + \frac{d\vec{\psi}_s}{dt} \qquad (8)$$

$$\vec{V}_r^r = R_r \vec{I}_r^r + \frac{d\vec{\psi}_r^r}{dt} \qquad (9)$$

To combine the circuits, the rotor voltage (notated with "*r*") has to be taken into the stator rotation speed reference frame. Per definition, it is referenced to the rotor frequency. (10) shows the Rotor Voltage matched to the base rotating speed:

$$\vec{V}_r = R_r \vec{I}_r + \frac{d\vec{\psi}_r}{dt} - j\omega_m \vec{\psi}_r \qquad (10)$$

With those relationships, the Space Vector circuit model can be found as shown in Figure 4. An additional voltage is used to represent the rotor voltage into the stator reference frame.

The Stator voltage taken from the circuit model is (11):

$$\vec{V}_s = R_s \vec{I}_s + L_{ls} \frac{d\vec{I}_s}{dt} + L_m \frac{d\vec{I}_s}{dt} + L_m \frac{d\vec{I}_r}{dt} \qquad (11)$$

C. Frequency domain model

With the space vector model as a base, the frequency domain model can be build. Laplace transformation is used to create (12), a function of the frequency variable *s*:

$$\vec{V}_s(s) = R_s \vec{I}_s + s\vec{I}_s(L_{ls} + L_m) + sL_m \vec{I}_r(s) \qquad (12)$$

The differential equation for $\vec{I}_r$ is shown in (13) and in frequency domain it can be represented as in (14) [7].

$$\vec{I}_r - \frac{d\vec{I}_r}{dt}\left(\frac{L_m}{j\omega_r(L_{lr} + L_m)}\right) = \frac{L_m \frac{d\vec{I}_s}{dt} - \vec{V}_r - j\omega_r L_m \vec{I}_s}{j\omega_r(L_{lr} + L_m) - R_r} \qquad (13)$$

$$\vec{I}_r(s) = \frac{\vec{V}_r(s) - L_m \vec{I}_s(s - j\omega_r)}{R_r + L_m(s - j\omega_r) - j\omega_r L_{lr}} \qquad (14)$$

The entire system in space vector and frequency domain is displayed in (16). The unknown rotor voltage, (15), is taken from chapter 6 in [7]:

$$\vec{V}_{rsc}(s) = \vec{I}_{rsoll} H(s - j\omega_s) - \vec{I}_r(H(s - j\omega_s) - jK_d) \qquad (15)$$

Where H is the *PI* Controller and jK_d describes the rotor current dynamics.

The approach used in [8] simplifies the controls to only one control loop. The whole DFIG rotor side converter (RSC) would have and inner and an outer control loop.

$$(16)$$

$$
\begin{aligned}
\vec{V}_s(s) &= R_s \vec{I}_s - s\vec{I}_s(L_{ls} + L_m) - sL_m \frac{\vec{V}_r + L_m \vec{I}_s(s - j\omega_r)}{R_r + L_m(s - j\omega_r) - j\omega_r L_{lr}} \\
&= R_s \vec{I}_s + s\vec{I}_s(L_{ls} + L_m) - \frac{sL_m^2 \vec{I}_s(s - j\omega_r)}{R_r + L_m(s - j\omega_r) - j\omega_r L_{lr}} + \frac{sL_m \vec{V}_r(s)}{R_r + L_m(s - j\omega_r) - j\omega_r L_{lr}} \\
&= \vec{I}_s \underbrace{\left(R_s + s\left((L_{ls} + L_m) - \frac{L_m^2(s - j\omega_r)}{R_r + L_m(s - j\omega_r) - j\omega_r L_{lr}}\right)\right)}_{Z_{ASM}} + \vec{V}_r(s)\frac{sL_m}{R_r + L_m(s - j\omega_r) - j\omega_r L_{lr}} \\
&= Z_{ASM} + \frac{\left(\vec{I}_{rsoll} H(s - j\omega_s) - \vec{I}_r\left(H(s - j\omega_s) - j(j\omega_r - s)\left((sL_{lr} + sL_m) - \frac{(sL_m)^2}{(sL_{ls} + sL_m)}\right)\right)\right)sL_m}{R_r + L_m(s - j\omega_r) - j\omega_r L_{lr}}
\end{aligned}
$$

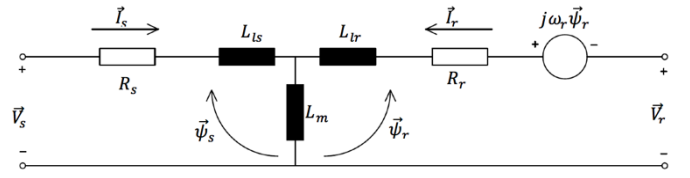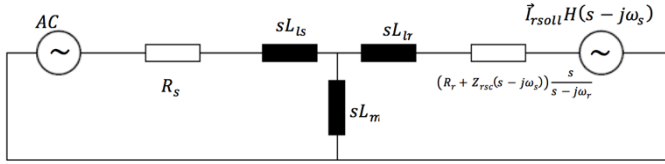Figure 5 Frequency domain single phase circuit without GSC

The next step is, to eliminate the need of the rotor current to calculate the impedance of the system. In [9] a DFIG developed, that has its rotor side calculated via the slip.

In [1] it's shown that a single-phase circuit can be used. Therefore, a current dependent voltage source with a corresponding impedance is used for the newly developed single phase circuit model. The voltage source (17) and the RSC impedance is (18) [7].

$$\vec{I}_{r*}H(s - j\omega_s) = \vec{V}_{rsc}(s) \tag{17}$$

$$Z_{rsc} = H(s - j\omega_s) - jK_d \tag{18}$$

Figure 5 shows the circuit model in frequency domain. The rotor side relates to the slip frequency and therefore, (20) is the Impedance of the DFIG without the grid side converter (GSC).

III. SIMULATION RESULTS

To see the frequency response, a bode plot of the impedance is made. To test the RSC, the control values for the PI controller are set to zero to see the difference in the behavior. The bode plot (Figure 6) of the impedance shows a peak at rotor frequency and, if the control values for the rotor side controller are not zero, a peak at stator frequency.

$$Z_{DGASM}(s) = \frac{Z_{ASMRSC}(s)(sL_t + Z_{gsc})}{Z_{ASMRSC}(s) + sL_t + Z_{gsc}} \tag{19}$$

The GSC is implemented the same way the RSC. It's connected via a transformer that is represented with an inductance. The circuit model is seen in Figure 7. The GSC connected in parallel, so the impedance of the whole system is (19).

Standard Control values are set for the machine, so a spike at rotor rotating speed and at stator frequency is expected. Also, different rotating speeds are simulated. As expected, a positive slip results in a spike lower than stator frequency and a negative slip shows a spike above start frequency. Figure 8 shows two examples, one for 90% rotating speed of the rotor and one for 110%. Comparing the bode plots of the DFIG with and without GSC shows, that the large impedance of the GSC filters out the visible effects of the induction machine and control. The control values of the GSC are changed in Figure 9 to see the effects.
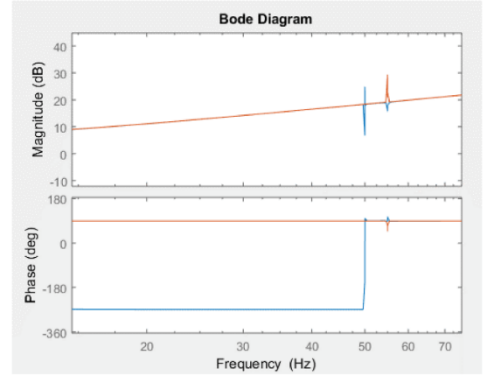

Figure 6 Bode Plot of DFIG without GSC; with control (blue) and without control (orange)
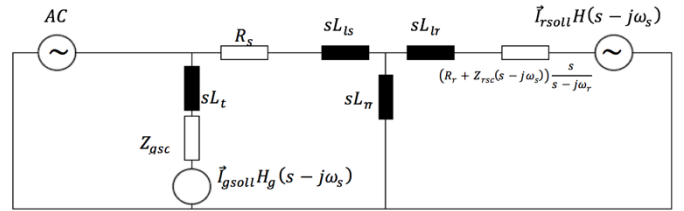

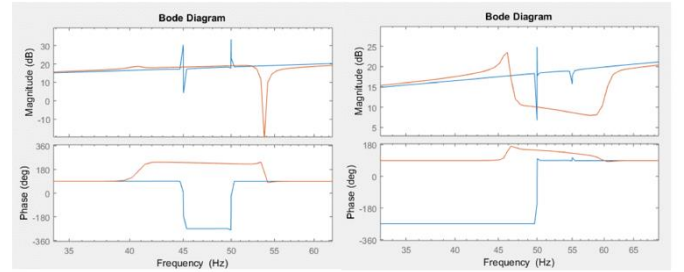Figure 7 Frequency domain single phase circuit with GSC

Figure 8 Bode plot of 90% rotor rotating speed on the left and 110% rotor rotating speed on the right; without GSC (blue) and with GSC (orange)
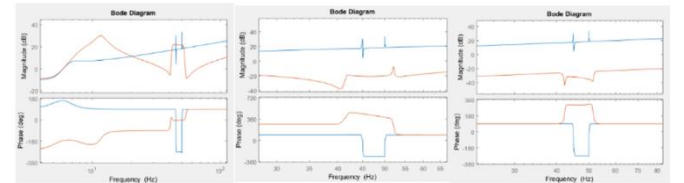

Figure 9 Different control values tested; on the left high values, in the middle weak control and on the right all values set to zero; without GSC (blue) and with GSC (orange)

$$Z_{ASMRSC}(s) = R_s + sL_{ls} + \cfrac{sL_m\left(sL_{ls} + \left(R_s + \left(K_P + \frac{K_P}{(s - j\omega_s)}\right) - j(j\omega_r - s)\left((sL_{lr} + sL_m) - \frac{(sL_m)^2}{(sL_{ls} + sL_m)}\right)\right)\frac{s}{s - j\omega_r}\right)}{\underbrace{sL_m + sL_{ls} + \left(R_s + \left(K_P + \frac{K_P}{(s - j\omega_s)}\right) - j(j\omega_r - s)\left((sL_{lr} + sL_m) - \frac{(sL_m)^2}{(sL_{ls} + sL_m)}\right)\right)\frac{s}{s - j\omega_r}}_{z_{rot}}} \tag{20}$$

While high control values distort the whole plot, also with weak control or without any control at all, the impedance has a strong impact on the results. So, depending on what the model should be used for, it could be advantageous to ignore the GSC in the model. The simplified DFIG model is complete. The next step is to connect it to an electrical network to see if it can be used in combination with electrical lines, cables or other equipment that shall be tested. Each network has a resonant frequency, this resonant frequency could match frequencies of the DFIG. The grid model here is a simple RCL circuit (21), that represents a power line and connected in row with the machine.

$$Z_{net}(s) = R + sL_{net} + \frac{1}{sC} \qquad (21)$$

The GSC is ignored in following bode plots and greyed out in Figure 10. It's shown with the Plots in Figure 11, that the grid does not affect the peaks of the DFIG. The grid impedance has a peak at its own resonant frequency. Again, positive and negative slip is tested.
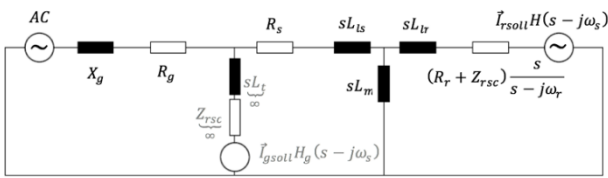

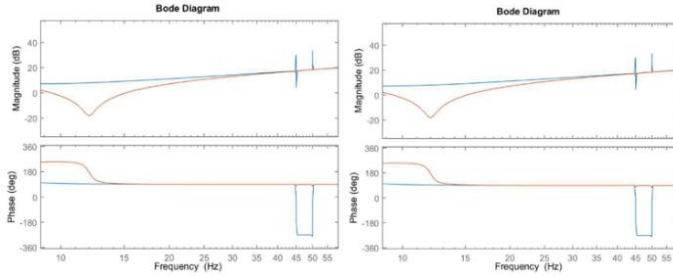Figure 10 Single phase DFIG with grid model; GSC greyed out

Figure 11 Figure 12 Bode plot of 90% rotor rotating speed on the left and 110% rotor rotating speed on the right; without transmission line (blue) and with transmission line (orange)

IV. CONCLUSION

The impedance based modeling of a doubly fed induction generator generates a simplified model. Basic behaviors can be observed but compared with a time-based simulation, some influential parts of the machine are left out. The two-mass swing system could interfere with other swing frequencies and the converters are treated as perfect voltage sources, which they are not in a real machine. Also, while the bode plots can be used for a quality analysis, they are not good for a quantity analysis because the spikes shown are not useful to determine the size of the effect.

REFERENCES

[1] Lakshan Piyasinghe, Zhixin Miao, Javad Khazaei, and Lingling Fan, "Impedance Model-Based SSR Analysis for TCSC Compensated Type-3 Wind Energy Delivery Systems", IEEE, 2015.

[2] Marc Cheah-Mane, Luis Sainz, Jun Liang, Nick Jenkins and Carlos E. Ugalde-Loo, "Criterion for the Electrical Resonance Stability of Offshore Wind Power Plants Connected through HVDC Links", IEEE, 2017.

[3] D. Johnson, "Origins of the Equivalent Circuit Concept: The Voltage-Source Equivalent", IEEE, 2003.

[4] Mahdi Debouza, Rachid Errouissi, Ahmed Al-Durra, S. M. Muyeen, "Design and implementation of a robust state-feedback control law for a grid-connected doubly fed induction generator wind turbine", IEEE, 2016.

[5] Miao, Lingling Fan Zhixin, "Modeling and Analysis of Doubly Fed Induction Generator Wind Energy Systems", Elsevier, 2015.

[6] Paul C. Krause, Oleg Wasynczuk, Scott D. Sudhoff, "Analysis of electric machinery and drive systems", New York: Wiley India Pvt. Ltd., 2011.

[7] Miao, Lingling Fan Zhixin, "Modeling and Analysis of Doubly Fed Induction Generator Wind Energy Systems", Elsevier, 2015.

[8] Li, Shuhui; Haskew, Timothy A., "Analysis of Decoupled d-q Vector Control in DFIG Back-to-Back PWM Converter", IEEE, 2007.

[9] Fan, Lingling; Miao, Zhixin, "Nyquist-Stability-Criterion-Based SSR Explanation for Type-3 Wind Generators", IEEE, 2013.